Diffusive Transport in Monolayer MoS_2: Role of Remote Coulomb Scattering

K. A. Khair and S. S. Ahmed
Department of Electrical and Computer Engineering
Southern Illinois University at Carbondale, 1230 Lincoln Drive, Carbondale, IL 62901, USA.
E-mail: khadijakhair@siu.edu

INTRODUCTION/BACKGROUND

2D MoS_2 with a finite bandgap looks promising as channel material for FETs. Recently, MoS_2 transistors operating at gigahertz frequencies (with a cutoff frequency of ~6 GHz) have been reported [1]. In monolayer MoS_2, the K-point direct bandgap is ~1.8 eV, the electron effective mass at the K point, $m_e^* = 0.48m_0$ and is isotropic in nature. Also, the two degenerate valleys at the K point are almost parabolic [2]. Nevertheless, electron mobility in monolayer MoS_2 is degraded by various scattering mechanisms. The 3-atom unit cell gives rise to nine phonon branches (3 acoustic and 6 optical) [3]. Recently, the role of individual scattering mechanisms in standalone monolayer MoS_2 was evaluated by calculating electron mobility (within an RTA framework) and from a comparative study it was concluded that mobility is mainly dominated by *ionized impurity scattering* [4][5]. Also, first-principles many-body calculations were done to obtain dielectric constant for monolayer MoS_2 [6]. For infinite layer separation, it was found that monolayer MoS_2 has a static dielectric constant of 1 whereas the previous studies reported the value in the range of 4.2-7.6.

In this work, using the recently reported value for the dielectric constant, we calculate the scattering rates in monolayer MoS_2 due to various a) intrinsic phonon, b) remote phonon, and c) remote Coulomb processes. We then study the electron transport in a monolayer MoS_2 based FET device employing a particle based Monte Carlo device simulator. Our results show that the total scattering rate is strongly dominated by remote coulomb scattering, which, when compared to the ballistic regime, degrades the drain current by ~78%.

MODEL

The simulated MoS_2 FET has a gate length of 14 nm, source-drain length of 20 nm and a width of 10 nm (Fig. 1). The channel thickness is ~0.65 nm (thickness of the MoS_2 layer) and the channel is undoped. We have used HfO_2 as top gate oxide with an equivalent oxide thickness (EOT) of ~2 nm. The MoS_2 channel sits on a SiO_2 buried oxide layer. Following scattering mechanisms have been included in the Monte Carlo transport kernel: acoustic (TA), acoustic (LA), optical (0th), optical (1st), polar optical, 0th and 1st order surface/remote optical in top gate oxide and buried oxide layers, and remote Coulomb in top gate oxide and buried oxide layers. A quasi-static assumption has been made for the holes. The Incomplete Lower-Upper (ILU) decomposition method has been employed for the solution of the Poisson equation.

RESULTS

The equilibrium simulations were benchmarked against an experimental device [1] giving rise to a sheet charge density of $\sim 2\times 10^{12}$ cm^{-2} at a $V_G = 2V$. Fig. 2 shows various scattering rates as function of electron energy. It is found that the influence of remote Coulomb and phonon scattering diminishes as the free carrier density increases in the channel region (Fig. 3). A pen picture of current degradation due to various scattering processes is depicted in Fig. 4. Finally, the calculated I_D-V_G and I_D-V_D characteristics are shown in Fig. 5. Calculation of various scattering rates as a function of carrier density and temperature, fine-tuning the MC simulator for atomicity and contact energetics, and the optimization of the FET for small off-current will be the subject of future study.

REFERENCES

[1] D. Krasnozhon et al., *Nano Lett.*, 14, p. 5905−5911, 2014.
[2] E. S. Kadantsev et al., *Solid State Commun*, 152, 10, pp. 909-913, 2012.
[3] Y. Cai et al., *Phys. Rev. B*, 89, p. 035438, 2014.
[4] K. Kaasbjerg et al., *Phys. Rev. B*, 85, 115317, 2012.
[5] N. Ma et al., *Phys. Rev. X*, 4, 011043, 2014.
[6] F. Huser et al., *Phys. Rev. B*, 88, 245309, 2013.

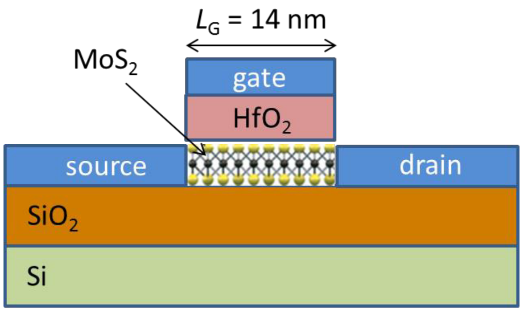

Fig. 1. Simulated MoS$_2$ FET.

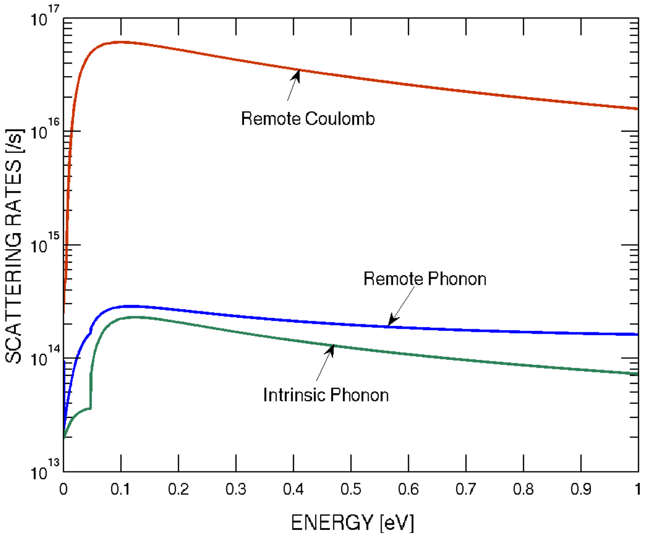

Fig. 2. Scattering rates (subcategories not shown).

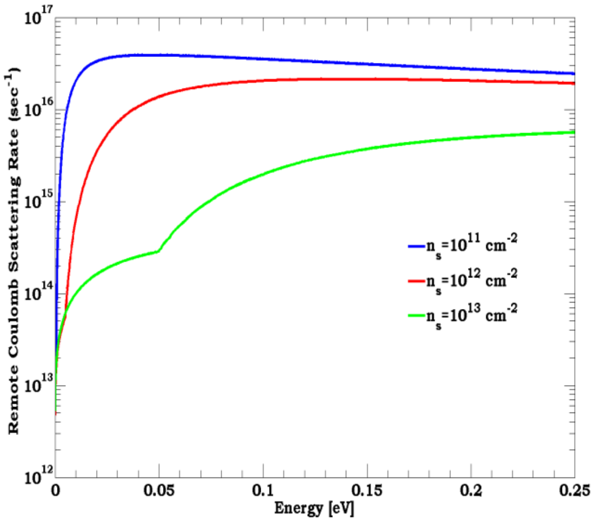

Fig. 3. Role of carrier density on remote Coulomb scattering.

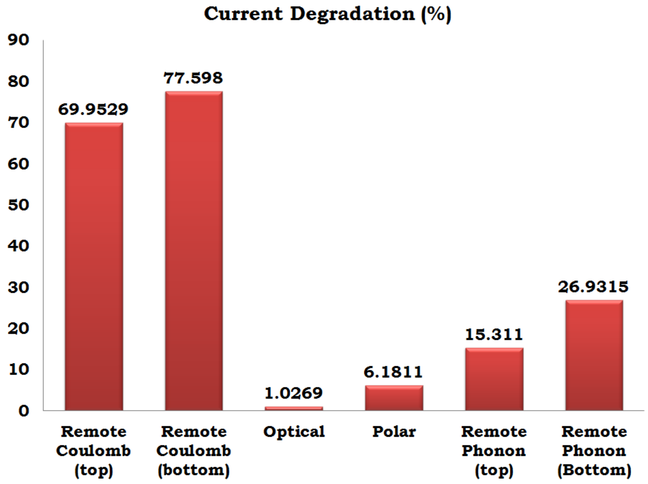

Fig. 4. Current degradation due to various scattering processes.

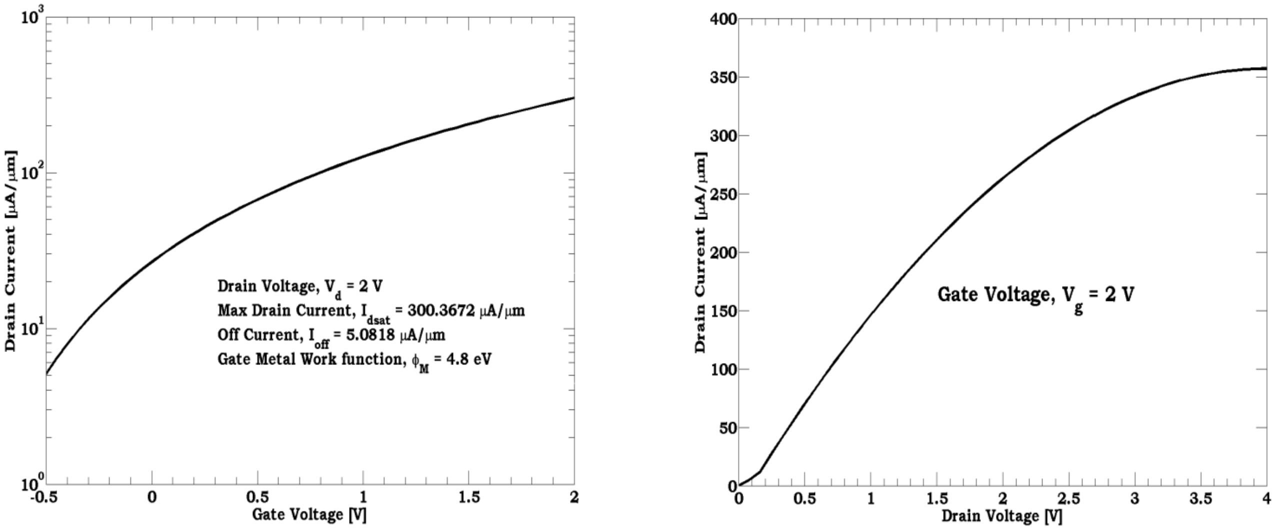

Fig. 5. The simulated I_D-V_G (left) and I_D-V_D (right) characteristics.